How to cite: *Angew. Chem. Int. Ed.* **2023,** *62,* e202217519
International Edition: doi.org/10.1002/anie.202217519
German Edition: doi.org/10.1002/ange.202217519

Cooperative Catalysis

A Practical and Robust Zwitterionic Cooperative Lewis Acid/Acetate/Benzimidazolium Catalyst for Direct 1,4-Additions

*Andreas C. Hans, Patrick M. Becker, Johanna Haußmann, Simon Suhr, Daniel M. Wanner, Vera Lederer, Felix Willig, Wolfgang Frey, Biprajit Sarkar, Johannes Kästner, and René Peters**

In memoriam of Professor Yoshito Kishi (13.4.1937–9.1.2023)

Abstract: A catalyst type is disclosed allowing for exceptional efficiency in direct 1,4-additions. The catalyst is a zwitterionic entity, in which acetate binds to Cu^{II}, which is formally negatively charged and serving as counterion for benzimidazolium. All 3 functionalities are involved in the catalytic activation. For maleimides productivity was increased by a factor >300 compared to literature (TONs up to 6700). High stereoselectivity and productivity was attained for a broad range of other Michael acceptors as well. The polyfunctional catalyst is accessible in only 4 steps from *N*-Ph-benzimidazole with an overall yield of 96 % and robust during catalysis. This allowed to reuse the same catalyst multiple times with nearly constant efficiency. Mechanistic studies, in particular by DFT, give a detailed picture how the catalyst operates. The benzimidazolium unit stabilizes the coordinated enolate nucleophile and prevents that acetate/acetic acid dissociate from the catalyst.

Introduction

Michael additions using 1,3-dicarbonyl pronucleophiles belong to the most important synthetic reactions in organic chemistry, as they allow for an atom-economic construction of 1,5-difunctionalized products.[1] Consequently, a number of valuable catalytic asymmetric studies has been reported.[1e,2] In this regard, great progress was also made in the simultaneous construction of adjacent quaternary and tertiary stereocenters.[1e,2] Still, for various classes of Michael acceptors frequently used in organic synthesis, surprisingly little data is available for catalytic asymmetric methods.

Maleimides represent one of these classes, for which synthetically attractive 1,4-additions of 1,3-dicarbonyls have been scarcely described to generate chiral highly enantioenriched succinimides with two adjacent stereocenters. This seems surprising, because succinimides represent an important structural motif in pharmaceutical sciences.[3] They are, for instance, used in drugs against HIV, as well as in antibacterial and antibiotic pharmaceuticals.[3,4]

Melchiorre described the use of cinchona alkaloids, which performed very well with *N*-benzylmaleimide.[5] Najera reported a C_2-symmetric bis(2-aminobenzimidazole) in the presence of trifluoroacetic acid to form products featuring adjacent quaternary and tertiary stereocenters in high yields with good diastereocontrol and high to excellent enantiocontrol.[6] While these two methods represent significant milestones, there are no highly enantioselective methods available allowing for turnover numbers (TONs) larger than 20.[5–7]

We report a novel, readily available Lewis acid/acetate/benzimidazolium catalyst that exhibits excellent activity and high stereoselectivity in 1,4-additions to maleimides, and also to other common Michael acceptors (Scheme 1, TONs up to 8500).[8,9]

Results and Discussion

Catalyst Development and Catalytic Activity

For catalyst development we chose the addition of ketoester **1a** to *N*-methylmaleimide **2A** as model reaction (Table 1). The investigation started with dimeric betaine catalyst **C1** (entry 1, 5 mol %), which in THF provided the addition product **3aA** in moderate yield and with moderate diaster-

[*] A. C. Hans, J. Haußmann, D. M. Wanner, V. Lederer, Dr. F. Willig, Dr. W. Frey, Prof. Dr. R. Peters
Universität Stuttgart, Institut für Organische Chemie
Pfaffenwaldring 55, 70569 Stuttgart (Germany)
E-mail: rene.peters@oc.uni-stuttgart.de
P. M. Becker, Prof. Dr. J. Kästner
Universität Stuttgart, Institut für Theoretische Chemie
Pfaffenwaldring 55, 70569 Stuttgart (Germany)
S. Suhr, Prof. Dr. B. Sarkar
Universität Stuttgart, Institut für Anorganische Chemie
Pfaffenwaldring 55, 70569 Stuttgart (Germany)

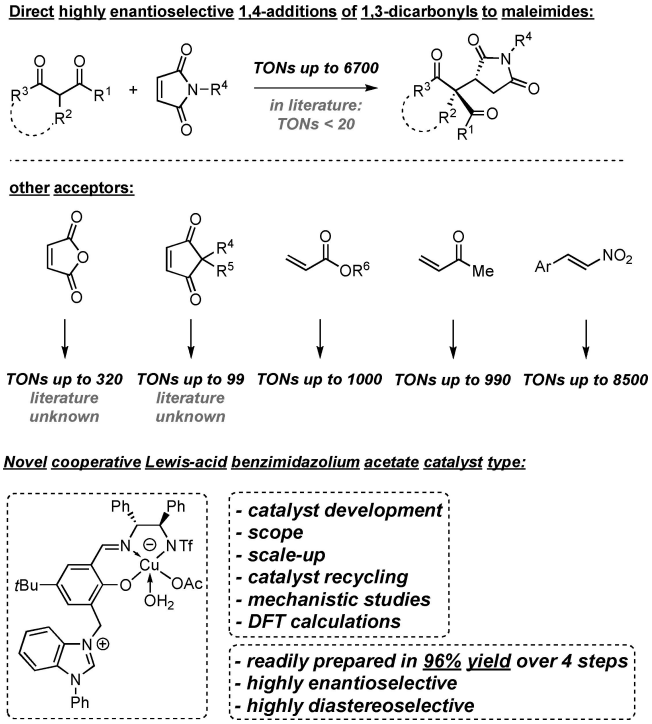

Scheme 1. Comparison of previous and this work.

eoselectivity, but promising enantiomeric excess.[10] Formally changing the imidazolium fragment to a benzimidazolium present in **C2** resulted in improved stereoselectivity (entry 2).[11–13]

Working at higher concentration, similar results were obtained with 1 mol % **C2** (entry 3). Protic additives were investigated to facilitate proton transfer steps that might potentially be a limiting factor. By adding water, improved yield, diastereo- and enantioselectivity were attained (entry 4). With the more acidic 1,1,1,3,3,3-hexafluoroisopropanol (HFIP) the effect was further amplified (entry 5). In that case, high performance was also possible with only 0.05 mol % **C2** (TON = 1680, entry 6).

To learn, if an aryloxide unit is required, we also used the simpler *N*-phenylbenzimidazolium catalyst **C3** which was found to be even more active and to allow for improved stereoselectivity (entries 7 and 8). Almost diastereomerically pure and highly enantiomerically enriched product was attained in high yield using as little as 0.02 mol % catalyst (TON = 4550, entry 8). With the similar catalysts **C4** and **C5** equipped with a more basic acac (entry 9) or a less basic chloride ligand (entry 10) the performance was found to be inferior. Other carboxylates like benzoate and pivaloate were slightly inferior in terms of enantioselectivity at low catalyst loadings (see Supporting Information).

The optimized conditions of entry 8 were also repeated replacing HFIP by acetic acid (entry 11) and in the absence of an additional proton source (entry 12). In both cases, yields and stereoselectivity were significantly lower. Under the optimized conditions catalyst **C3** allows for TONs that are more than two orders of magnitude higher than with previously reported catalyst systems for this reaction type.

The structure of **C3** was confirmed by X-ray crystal structure analysis (see Supporting Info).[14] It shows that acetate binds to Cu^{II}. Formally, a negatively charged copper center is the internal counterion of the benzimidazolium moiety in **C3**. A water molecule adopts a fifth coordination site.

Reaction Scope of the 1,4-Addition to Maleimides

Several pronucleophiles **1** were exposed to the optimized reaction conditions (Table 2). Various ester moieties that would allow for orthogonal ester cleavage protocols,[15] were well tolerated. Next to the methyl and ethyl ester (entries 1–3) also *tert.*-butyl (entry 4), benzyl (entry 5) and allylic esters (entry 6) allowed for TONs around 1000 or above. The highest productivity was attained with the ethyl ester **1b** with TONs of 4900 and 6700 (entries 2 and 3). In addition, propargyl and neopentyl esters were used (entries 7 and 8).

Also, with cyclohexanone **1h** high diastereo- and enantioselectivity was found (entry 9). With the benzannulated **1i**, a reaction temperature of 0 °C was used because diastereocontrol turned out to be challenging (entry 10). Still high yields and enantioselectivity were achieved. Acyclic β-ketoesters could also be employed and gave high yields and stereoselectivities (entries 11–13). Due to their higher flexibility these substrates are less acidic.[2c] Arguably for that reason, catalyst loadings needed to be higher than with cyclic substrates and **C4** bearing the more basic acac ligand was superior.

Due to the importance of fluoro substituents in pharmaceuticals and for many other applications, the use of the α-fluorinated β-ketoester **1m** is of note (entry 14).[16] Tan et al. used a guanidine catalyst to prepare the addition products in excellent yield and with excellent stereocontrol achieving a TON of 20.[17,18] With **C3**, high yield, enantio- and diastereoselectivity could also be accomplished with 0.5 mol % catalyst.

In addition to β-ketoesters, the method also accommodates other 1,3-dicarbonyl pronucleophiles, for instance lactone **1n**, diketone **1o** and lactam **1p** (entries 15–17). For the synthesis of ketolactone **3nA** diastereoselectivity turned out to be particularly difficult to control though. For that reason, the addition was conducted at −20 °C to form the product in good yield and with high enantioselectivity (entry 15). Surprisingly, diastereocontrol was much better for the structurally similar diketone **1o** (entry 16) and lactam **1p** (entry 17).

The absolute configurations of products **3fA**, **3gA**, **3iA**, **3jA** and **3oA** were determined by X-ray analysis suggesting the general configuration of the products as depicted in Table 2.[14] In contrast, for ketolactone **3nA**, the relative configuration is different as revealed by X-ray crystal structure analysis.[14] In this case, the stereocenter generated at the pronucleophile is opposite to the one shown in Table 2.

Next to the different 1,3-dicarbonyl pronucleophile types, we also studied different maleimide substrates **2** with varying *N*-substituents as well as maleic anhydride **4**

Table 1: Optimization of the 1,4-addition of **1a** to maleimide **2A**.

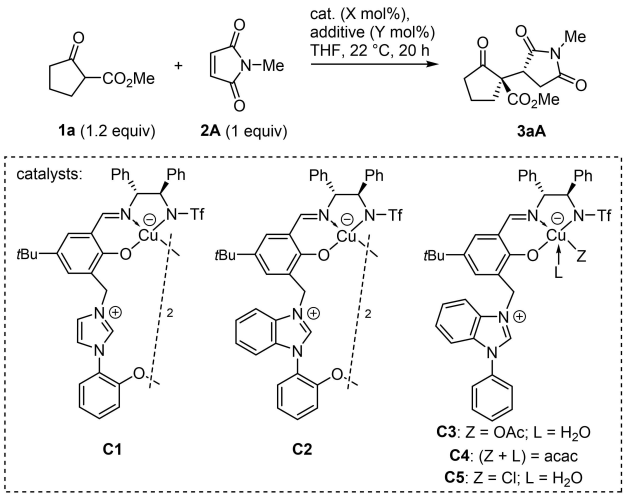

#	C (X)	additive (Y)	conc.	y [%][a]	dr[b]	ee [%][c]	TON
1	**C1** (5.0)	–	0.5 M	69	79:21	84	14
2	**C2** (5.0)	–	0.5 M	57	93:7	91	11
3	**C2** (1.0)	–	2 M	58	93:7	91	58
4	**C2** (1.0)	H_2O (25)	2 M	78	96:4	93	78
5	**C2** (1.0)	HFIP (25)	2 M	88	98:2	96	88
6	**C2** (0.05)	HFIP (25)	2 M	84	96:4	90	1680
7	**C3** (0.05)	HFIP (25)	2 M	99	99:1	97	1980
8	**C3** (0.02)	HFIP (25)	2 M	91	98:2	94	4550
9	**C4** (0.05)	HFIP (25)	2 M	93	99:1	96	1860
10	**C5** (0.10)	HFIP (25)	2 M	26	93:7	91	260
11	**C3** (0.05)	HOAc (25)	2 M	55	92:8	80	1100
12	**C3** (0.05)	–	2 M	34	78:22	80	680

[a] Yield determined by ^{1}H NMR using an internal standard. [b] Determined by ^{1}H NMR of the crude mixture. [c] Determined by HPLC.

(Table 3). Besides the N–Me derivative **2A**, the unprotected maleimide **2C** was well tolerated and allowed for a TON of 485 and excellent stereoselectivity (entry 1). High activity was also attained with the *N*-benzyl (TON 830, entry 2) and the *N*-phenyl substituted substrates (TON 720, entry 3). Moreover, both Boc (*tert.*-butyloxycarbonyl, entry 4) and Cbz (benzyloxycarbonyl, entry 5) protected substrates worked well.

The absolute configuration of product **3aC** derived from the parent maleimide was also determined by X-ray crystal structure analysis and again fits to the general configuration of the products depicted in Tables 2 and 3.[14]

Surprisingly, highly enantioselective catalytic asymmetric 1,4-additions of 1,3-dicarbonyls to maleic anhydride **4** are unknown. Application of our standard conditions resulted in a slower reaction as compared to most maleimides (entry 6). Nevertheless, the addition product was obtained in good yield and a TON of 320 with high stereoselectivity. The absolute configuration of **5** could again be determined by X-ray analysis[14] and is in agreement with the expectations.

A further challenge was the use of maleimide **2G** bearing a *tert.*-butyl substituent in *ortho*-position of the *N*-aryl moiety thus limiting the rotational freedom of the aryl substituent (Scheme 2). Despite the fact that the product now also contains the additional element of axial chirality ($N–C_{aryl}$ as chirality axis), a single diastereomer was detected

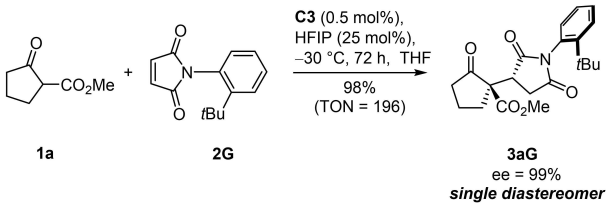

Scheme 2. Atroposelective synthesis of diastereomerically pure product **3aG**.

out of four possible. In a previous study, the corresponding ethyl ester could be formed with a TON of 5, 50 % ee and a dr of 8:1 using a biscinchona alkaloid catalyst.[19,20] The absolute configuration of **3aG** was resolved by X-ray analysis.[14] Both stereocenters have again an (*R*)-configuration, whereas the product is (R_a) configured regarding the chirality axis.

Application to Other Michael Acceptors

Further Michael acceptors were then studied to see if the new catalyst system is of wider utility. Remote stereocontrol was achieved for 4-cyclopenten-1,3-dione derivative **6**, featuring a prochiral quaternary C atom (Scheme 3). Upon

Table 2: Application of different pronucleophiles **1**.

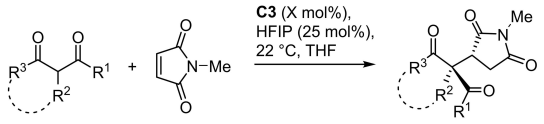

1 **2A** **3_A**

#	**1**	**3_A**	X mol %	TON	y [%][a]	dr[b]	ee [%][c]
	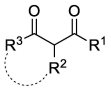						
	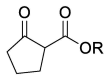						
1	R: Me	**1a**	**3aA**	0.05	1980	97	99:1	97
2	R: Et	**1b**	**3bA**	0.02	4900	98	99:1	98
3	R: Et	**1b**	**3bA**	0.01	6700	67	95:5	96
4	R: *t*Bu	**1c**	**3cA**	0.10	960	96	95:5	95
5	R: Bn	**1d**	**3dA**	0.025	3560	89	98:2	>99
6	R: $CH_2CH{=}CH$	**1e**	**3eA**	0.025	3720	93	99:1	97
7	R: $CH_2C{\equiv}CH$	**1f**	**3fA**	0.05	1880	94	99:1	97
8	R: CH_2*t*Bu	**1g**	**3gA**	0.10	700	70	99:1	96
9[d]	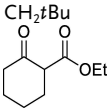	**1h**	**3hB**	0.5	156	78	99:1	93
10[f,e]	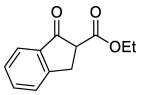	**1i**	**3iA**	0.5	192	91	80:20	89
	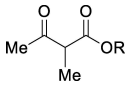						
11[f,g]	R: Et	**1j**	**3jA**	2.5	38	94	91:9	91
12[f,g]	R: Bn	**1k**	**3kA**	2.5	37	92	87:13	92
13[f,g]	R: $CH_2CH{=}CH$	**1l**	**3lA**	2.5	39	97	90:10	91
14	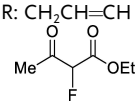	**1m**	**3mA**	0.5	178	89	96:4	95
							
15[f,h,i]	X: O, R: Me	**1n**	**3nA**	2.0	41	82	74:26	89
16[e]	X: CH_2, R: Me	**1o**	**3oA**	2.0	45	90	93:7	93
17[f,e,j]	X: NMe, R: OMe	**1p**	**3pA**	1.0	97	97	88:12	93

[a] Yield of almost diastereopure product after column chromatography. [b] Determined by ^{1}H NMR /GC of the crude mixture. [c] Determined by HPLC/GC. [d] *N*-Benzylmaleimide was used. [e] The reaction was performed at 0 °C. [f] Product isolated as a diastereomeric mixture. [g] **C4** was used as catalyst. [h] The reaction was performed at −20 °C. [i] The relative configuration of this product is different for this product, see text. [j] The configuration is unknown.

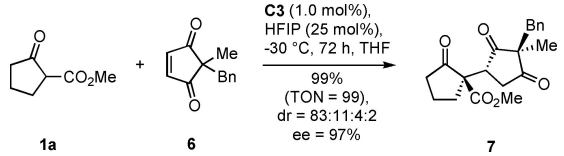

1a **6** **7**

Scheme 3. Enantio- and diastereoselective 1,4-addition to 1,3-diketone **6** containing a prochiral quaternary C atom.

1,4-addition a third stereocenter is created by desymmetrization. Four enantiomeric pairs of diastereomers can thus be formed. The major diastereomer of **7** was produced with good diastereo- and high enantiocontrol.[21] The configuration of the diketo substituted quaternary stereocenter was determined by NOESY (see Supporting Information).

Quite rare in literature are also highly enantioselective catalytic asymmetric 1,4-additions to acrylic esters and TONs >20 were, to our knowledge, not reported for highly enantioselective reactions.[22,23] Also for 1,4-additions of 1,3-dicarbonyls to methyl vinyl ketone **9** (MVK), relatively few highly enantioselective methods are currently available.[25,22] To our knowledge, TONs were in all cases below 100 using ketoester substrates.

To achieve proper reactivity hexafluoroisopropyl acrylate **8** was employed (Scheme 4). To form product **10** with useful enantioselectivity the reaction was performed at −40 °C. 0.1 mol % of **C3** provided the 1,4-adduct in quantita-

Table 3: Application to different maleimides and malic anhydride.

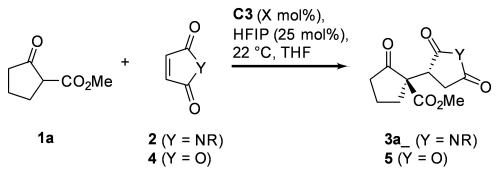

#	R	2/4	3 *a*_/5	X mol %	TON	y [%][a]	dr[b]	ee [%][c]
1	N–H	**2C**	**3aC**	0.2	485	97	99:1	99
2	N–Bn	**2B**	**3aB**	0.1	830	83	99:1	97
3	N–Ph	**2D**	**3aD**	0.1	720	72	98:2	97
4	N–Boc	**2E**	**3aE**	1.0	98	98	95:5	91
5	N–Cbz	**2F**	**3aF**	1.0	93	93	95:5	89
6	O	**4**	**5**	0.25	320	80	97:3	93

[a] Yield of the almost diastereopure product after column chromatography. [b] Determined by ^{1}H NMR /GC of the crude mixture. [c] Determined by HPLC/GC.

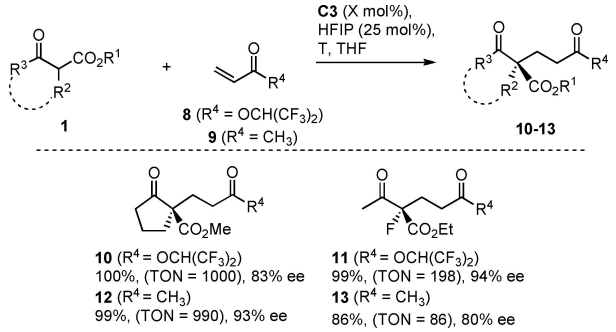

Scheme 4. Enantioselective 1,4-additions to acrylate **8** and MVK.

tive yield (TON = 1000) with 83 % ee.[14] Similarly, the protocol was applied to the acyclic α-fluorinated ketoester **1m**.[24] With 0.5 mol % of catalyst also a nearly quantitative yield (TON = 198) and high enantioselectivity (94 % ee) was attained for **11**.

The reaction between cyclic ketoester **1a** with MVK was best performed at −30 °C (Scheme 4). **12** was isolated in nearly quantitative yield (TON = 990) with 93 % ee. The acyclic α-fluorinated ketoester **1m** reacted slower with MVK thus 1.0 mol % of catalyst were used (TON = 86, 80 % ee).[24]

Moreover, we examined nitroolefins **14** as Michael acceptors (Table 4).[26] A maximum TON of 182 was previously achieved for the synthesis of the depicted diastereomer, which is otherwise difficult to get.[10a] In comparison, **C3** offered a significantly higher activity and TONs up to 8500 were attained (entry 2).

Scale-Up Experiments and Catalyst Recycling

The addition reaction of ketoester **1a** to *N*-methylmaleimide **2A** was also investigated on gram scale (Scheme 5, *top*). With 2.1 mg of catalyst **C3** (0.05 mol %), 1.44 g of product **3aA** was isolated (TON 1820, yield 91 %, dr = 99:1, ee = 97 %). Another gram scale experiment was performed with MVK (Scheme 5, *bottom*). 1.04 g of **12** was isolated (TON 980, yield 98 %) with high enantiomeric excess (*ee* = 91 %) using 4.2 mg of catalyst (0.1 mol %).

Catalyst recycling was studied for the model reaction using 0.1 mol % of **C3** (Table 5). After each run the catalyst was separated by filtration over silica gel. In total 10 runs were performed with the same catalyst batch with only a minor decrease in ee. 1.40 g of the chiral addition product was formed with as little as 0.42 mg of the catalyst demonstrating the robustness of the catalytic system.

Table 4: Enantio- and diastereoselective 1,4-addition to nitroolefins.

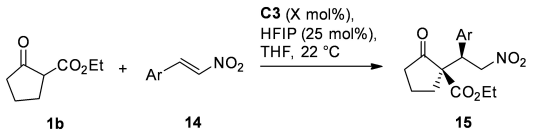

#	Ar	15	X mol %	TON	y [%][a]	dr[b]	ee [%][c]
1	Ph	**15a**	0.02	5000	100	92:8	91
2	Ph	**15a**	0.01	8500	85	83:17	88
3	*p*-Me-Ph	**15b**	0.05	1980	99	87:13	95
4	*p*-Cl-Ph	**15c**	0.10	820	82	90:10	95
5	*p*-NO_2-Ph	**15d**	0.02	4450	89	89:11	94
6	*o*-NO_2-Ph	**15e**	0.5	>198	>99	95:5	95

[a] Yield of the isolated product after column chromatography. [b] Determined by ^{1}H NMR of the crude mixture. [c] Determined by HPLC.

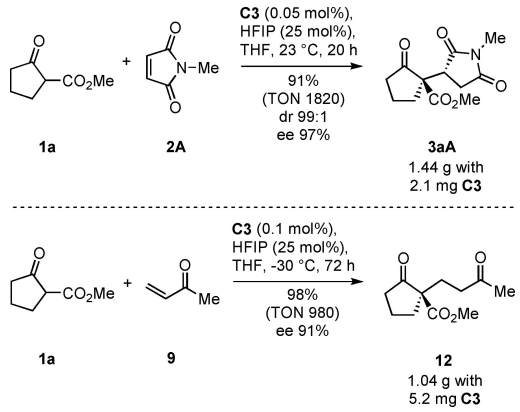

Scheme 5. Scale-up experiments.

Table 5: Catalyst recycling experiments.

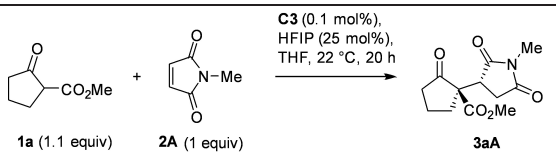

Run	y [%][a]	dr[b]	ee [%][c]
1	>99	99:1	97
2	>99	99:1	96
3	>99	99:1	96
...			
10	>99	99:1	94

[a] Yield determined by ^{1}H NMR using an internal standard. [b] Determined by ^{1}H NMR of the crude mixture. [c] Determined by HPLC.

Control Experiments

To evaluate which catalyst functionalities are essential, several control experiments were performed (Table 6). Catalyst **C6** lacking the benzimidazolium moiety showed poor catalytic activity and stereoselectivity (entry 1). In the presence of NaOAc, the activity was improved, but stereoselectivity remained low (entry 2). Combining **C6** with benzimidazolium salts **B1** and **B2** in the presence of NaOAc did not result in improvements (entries 3 and 4) compared to entry 2. This suggests that all three functionalities—Lewis acid, benzimidazolium and acetate—combined in one catalyst molecule are crucial for the efficiency of the reported system.

Kinetic Investigations

Determination of the empirical rate law was conducted by variable time normalization analysis (see Supporting Information).[27] The model reaction was studied via NMR using catalyst **C3**. The best fit for the normalization of the time scale axis was achieved for the following Equation (1):

$$r = k_{obs}\ [\mathbf{C3}]^{0.95}\ [\mathbf{2A}]^{1.0}\ [\mathbf{1a}]^{-0.05}\ [\mathrm{HFIP}]^{0.75}\ [\mathbf{3aA}]^{-0.05} \quad (1)$$

The first order in catalyst suggests that a single catalyst molecule is involved in the rate limiting step. To probe this interpretation, we studied a possible non-linear effect.[28] As expected, a linear dependence between catalyst ee and product ee values was determined (see Supporting Information). The zero order in ketoester might indicate a substrate saturation. This in combination with the orders in maleimide might be interpreted by a limiting C–C bond formation step.

Table 6: Control experiments.

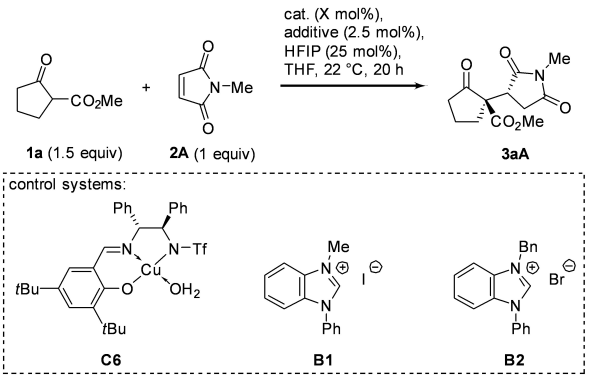

#	cat.	X mol%	additive	y [%][a]	dr[b]	ee [%][c]
1	**C6**	2.5	–	14	51:49	13
2	**C6**	2.5	NaOAc	92	47:53	7
3	**C6** & **B1**	2.5 & 2.5	NaOAc	78	44:56	3
4	**C6** & **B2**	2.5 & 2.5	NaOAc	87	47:53	7

[a] Yield determined by ^{1}H NMR using an internal standard. [b] Determined by ^{1}H NMR/GC of the crude mixture. [c] Enantiomeric excess of the major diastereomer determined by HPLC.

EPR Studies

C3 displays an axial spectrum in frozen THF, with $g_{\parallel} = 2.253$, $g_{\perp} = 2.053$; $A_{\parallel} = 501$ MHz (0.0167 cm^{-1}), $A_{\perp}$ 48 MHz and hence a ratio of $g_{\parallel}/A_{\parallel} = 135$ cm (see Supporting Information). According to the Peisach/Blumberg maps,[29] these values indicate an equatorial N_2O_2 coordination plane with additional axial coordination and are thus in accordance with the crystallographically determined molecular structure shown above. The ratio of $g_{\parallel}/A_{\parallel}$ indicates only little distortion in the equatorial plane.[30] Similar values have also been reported for octahedral Cu^{II} complexes with axial elongation.[31,32]

Computational Studies

To gain more insight into the reaction mechanism and to find an explanation for the high stereoselectivity, we performed density functional theory (DFT) calculations on the B3LYP-D3(BJ)/def2-TZVP/COSMO (THF) level of theory on PBEh-3c-D3(BJ)/def2-mSVP geometries (for computational details see Supporting Information).[33] The crystal structure of **C3** (see Supporting Info) served as a starting point for all further generated geometries.

At first, the solution state structure of the catalyst was investigated. To identify the catalytically active species, we simulated a large range of possible ligand combinations: the water molecule and the acetate anion of **C3** were replaced by either THF, HFIP, or the deprotonated HFIP anion. The comparison of the investigated adducts (summarized in the Supporting Information) indicates that an anionic ligand, e.g., acetate, in the coordination sphere of the Cu^{II} center significantly stabilizes the system. However, according to our DFT results, an HFIP ligand replaces the water molecule of **C3**, forming **C3-HFIP** (see Supporting Information). The H_2O/HFIP exchange is slightly endergonic by 2.7 kJ mol^{-1}. Nevertheless, **C3-HFIP** is abundant in solution, because the high excess of HFIP pushes the equilibrium. Due to an additional O(Tf)···Cu^{II} contact (3.01 Å, sum of van-der-Waals-radii: 2.92 Å[34]), **C3-HFIP** possesses a N_2O_2 coordination vicinity with additional axial coordination around the copper center, which agrees with the EPR results (vide supra).

Based on the described experimental and computational results, we propose the simplified catalytic cycle shown in Scheme 6.

The quantum chemical investigation of the catalytic reaction predicts a reaction energy profile shown in Figure 1 with a thermodynamic driving force of 28.8 kJ mol^{-1}.

To initiate the catalytic cycle, **1a** replaces HFIP. The next step is a proton transfer of the coordinated ketoester to acetate, to form **I**. The enolate acts as a bidentate ligand. Its orientation at the copper center in **I** has nearly no impact on the system's energy (20.2 kJ mol^{-1} vs. 20.4 kJ mol^{-1} for the two orientations). In each case, Cu^{II} possesses a distorted square pyramidal coordination vicinity with an ester group binding to the axial position.[35]

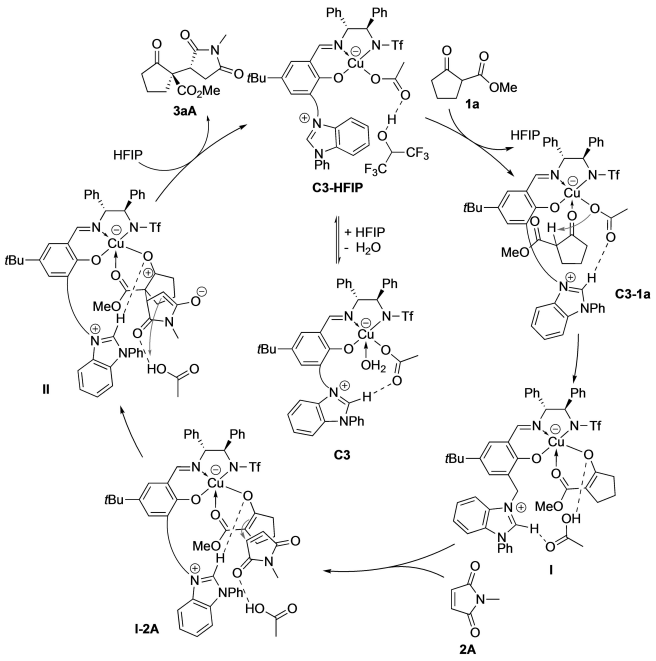

Scheme 6. Proposed simplified catalytic cycle.

As next step, **2A** coordinates to **I**, forming **I-2A**. DFT predicts a significant dependence of the reaction energy of that step on the stereoisomer formed (see Figure 1). The catalyst's backbone shields one side of the enolate. While in **I** the orientation of the enolate has nearly no impact on the free energy, for **I-2A** the *Re*-side reacts preferably due to steric repulsion of the enolate/maleimide-complex with the catalyst's chiral backbone preventing comparable conformations for a *Si*-side attack. Moreover, in the reactive configurations the less electron-rich carbonyl-oxygen of the ester group occupies the axial Cu^{II} coordination side.

According to DFT, the C–C bond formation from **I-2A** to **II** is rate determining. That agrees with the interpretation of the kinetic investigations (vide supra). The C–C bond formation step has a barrier of 79.6 kJ mol^{-1} for the main (*R*,*R*)-product, which agrees well with an apparent barrier height of 77.1 kJ mol^{-1} that can be deduced form the kinetic data (for details see Supporting Information).

During the C–C-bond formation two stereocenters are formed. Hence, four different configuration isomers had to be considered. The nascently formed acetic acid activates **2A** in all cases. Contra-intuitively, the maleimide's α-C is more reactive in the major pathway for inductive effects (see the Supporting Information for details). The transition state for the (*R*,*R*)-product (see Supporting Information) is energetically most favored, since **2A** is activated by the acetic acid, the nucleophile is stabilized by a hydrogen bond to the catalyst, and steric hindrance between the substrates and the catalyst's backbone is minimized. In the (*R*,*S*)-transition state (see Supporting Info) the acetic acid molecule and the C(2)-H of the benzimidazolium moiety form a defined hydrogen-bond network together with **2A**; for all other configu-

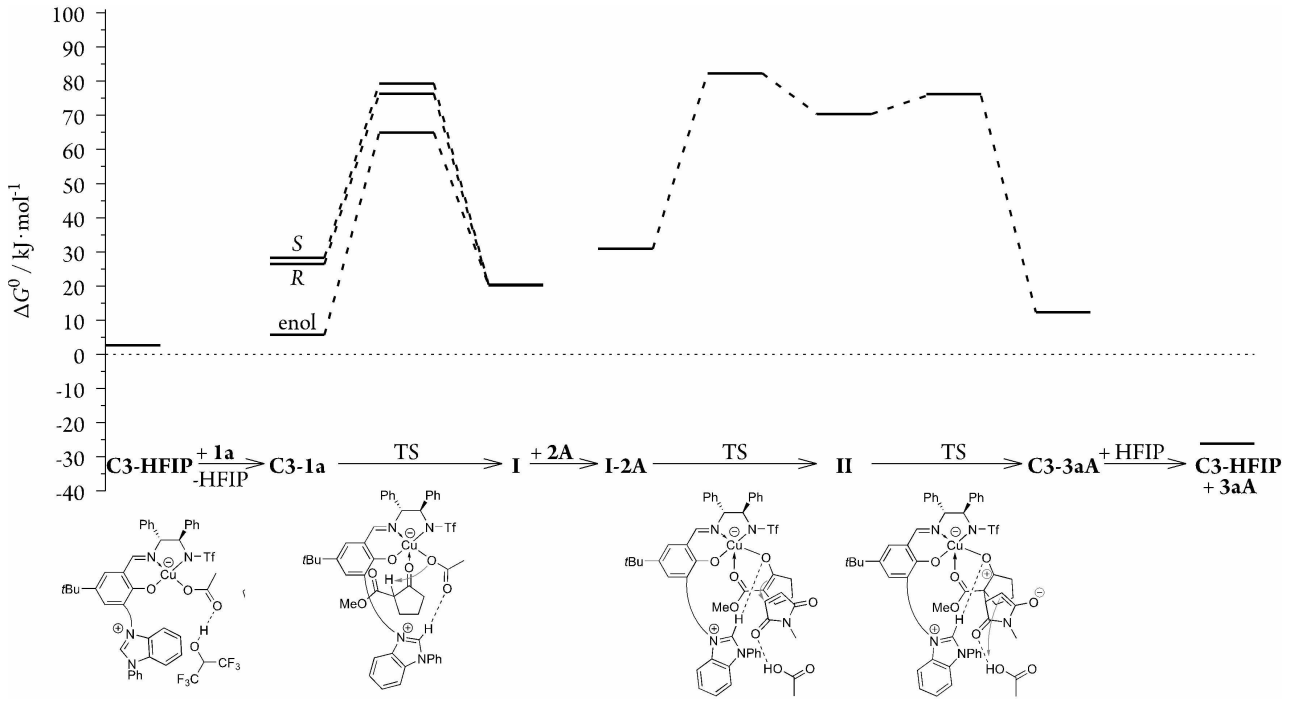

Figure 1. Free energy profile of the proposed catalytic cycle (see Scheme 6). **C3** was chosen as reference state ($\Delta G^0 = 0$ kJ mol^{-1}).

rations no such assembly could be found. Instead, the nucleophile is stabilized by a hydrogen bond from the benzimidazolium unit to the enolate O-atom. The significant Gibbs free-energy differences (see Supporting Information) of 11.2 kJ mol^{-1} (*R*,*S*), 38.1 kJ mol^{-1} (*S*,*R*) and 29.5 kJ mol^{-1} (*S*,*S*) compared to (*R*,*R*) result in a predicted dr of 99:1 and an ee >99 % for the (*R*,*R*)-product. That agrees reasonably with the results in Table 2.

Besides for forming the actually catalytically active species, we found HFIP to be necessary for product/catalyst-dissociation: coordination of HFIP to **C3–3aA** breaks the hydrogen bond between the acetate anion and the benzimidazolium's C(2)-H. Thereby, the latter one could rotate around the C–N-bond to the bridging methylene group opening space for nucleophilic attack of the acetate anion at the Cu^{II} center whereby **3aA** is replaced (for details see Supporting Information).

Conclusion

In summary, we have developed a new catalyst type that achieves unprecedented productivity for a number of different 1,4-addition types. Diverse classes of 1,3-dicarbonyl pronucleophiles and Michael acceptors have been coupled. Turnover numbers of up to 6700 for maleimides could be achieved, which corresponds to an increase by a factor of >300 compared to catalyst systems known from the literature. For nitroolefins TONs up to 8500 were accomplished. Synthetically very attractive productivities were also found for other common electron poor olefins. The polyfunctional catalyst system uses the cooperation of a formally negatively charged Cu^{II} center with its acetate ligand, a benzimidazolium unit in the catalyst periphery, and hexafluoroisopropanol as a catalytic additive. Control experiments show that cooperation between these components is essential for high efficiency and that the interplay of Lewis acid and benzimidazolium must be intramolecular to be effective. Spectroscopic and kinetic studies provide a mechanistic picture in which a monomeric catalyst unit forms a Cu enolate with the ketoester substrate by aid of acetate. Detailed DFT studies strongly support a cooperative mode of action and show that the nascently formed acetic acid activates the Michael acceptor by a hydrogen bond. The C(2)–H bond of the benzimidazolium acts as H-bond donor to stabilize the nucleophile. By controlling the spatial arrangement of both substrates during their concurrent activation within the chiral environment of the catalyst sphere, high to excellent stereoselectivities could be achieved. The catalyst is easily accessible in 4 steps from *N*-phenylbenzimidazole in an overall yield of 96 %. It is stable during catalysis and could therefore be recovered and reused numerous times with virtually unchanged performance. We believe that the reported study may also be of technical interest due to its various practical benefits.

Acknowledgements

Funded by the Deutsche Forschungsgemeinschaft (DFG, German Research Foundation) - project-ID 310990893, project-ID 358283783-SFB 1333/2 2022, no INST 40/575-1 FUGG (JUSTUS 2 cluster). We acknowledge support by

the state of Baden-Württemberg through bwHPC and thank the analytical service of the Institute of Organic Chemistry at the University of Stuttgart for their support. Moreover, we thank M.Sc. Fridolin Hennhöfer (Sarkar group, Universität Stuttgart) for his support during EPR measurements. P.M.B. acknowledges financial support in the form of a PhD scholarship from the Studienstiftung des Deutschen Volkes (German National Academic Foundation). J.H. acknowledges financial support by a Deutschlandstipendium. Open Access funding enabled and organized by Projekt DEAL.

Conflict of Interest

The authors declare no conflict of interest.

Data Availability Statement

The data that support the findings of this study are available in the Supporting Information of this article.

Keywords: Asymmetric Catalysis · Cooperative Catalysis · Copper Enolates · Hydrogen Bonds · Multifunctional Catalysts

[1] a) Review: S. Benetti, R. Romagnoli, *Chem. Rev.* **1995**, *95*, 1065–1114; b) J. C. Stowell, *Carbanions in Organic Synthesis*, Wiley, New York, **1979**; c) P. Perlmutter, *Conjugate Addition Reactions in Organic Synthesis*, Pergamon, Oxford, **1992**; d) H. O. House, *Modern Synthetic Reactions*, W. A. Benjamin, New York, **1972**; e) E. Reyes, U. Uria, J. L. Vicaro, L. Carrillo, *Org. React.* **2016**, *90*, 1–898.

[2] a) V. Andrushko, N. Andrushko, *Stereoselective Synthesis of Drugs and Natural Products, Vol. 1*, Wiley, New York, **2013**; b) H. Pellissier, *Adv. Synth. Catal.* **2015**, *357*, 2745–2780; c) T. Govender, P. I. Arvidsson, G. E. M. Maguire, H. G. Kruger, T. Naicker, *Chem. Rev.* **2016**, *116*, 9375–9437; d) D. Sun, S. Yang, F. Xinqiang, *Org. Chem. Front.* **2020**, *7*, 3557–3577; e) A. N. Reznikov, Y. N. Klimochkin, *Synthesis* **2020**, *52*, 781–795; f) T. Das, S. Mohapatra, N. P. Mishra, S. Nayak, B. P. Raiguru, *ChemistrySelect* **2021**, *6*, 3745–3781; g) H. Li, Y. Wang, L. Tang, F. Wu, X. Liu, C. Guo, B. M. Foxman, L. Deng, *Angew. Chem. Int. Ed.* **2005**, *44*, 105–108; *Angew. Chem.* **2005**, *117*, 107–110; h) F. Wu, R. Hong, J. Khan, X. Liu, L. Deng, *Angew. Chem. Int. Ed.* **2006**, *45*, 4301–4305; *Angew. Chem.* **2006**, *118*, 4407–4411; i) F. Wu, H. Li, R. Hong, L. Deng, *Angew. Chem. Int. Ed.* **2006**, *45*, 947–950; *Angew. Chem.* **2006**, *118*, 961–964; j) B. Huang, C. Li, H. Wang, C. Wang, L. Liu, J. Zhang, *Org. Lett.* **2017**, *19*, 5102–5105.

[3] a) Review: P. Chauhan, J. Kaur, S. S. Chimni, *Chem. Asian J.* **2013**, *8*, 328–346; b) R. Shintani, W.-L. Duan, T. Hayashi, *J. Am. Chem. Soc.* **2006**, *128*, 5628–5629; c) M. Weber, W. Frey, R. Peters, *Angew. Chem. Int. Ed.* **2013**, *52*, 13223–13227; *Angew. Chem.* **2013**, *125*, 13465–13469.

[4] a) K. Tang, J.-T. Zhang, *Neurol. Res.* **2002**, *24*, 473–478; b) C. Freiberg, H. P. Fischer, N. A. Brunner, *Antimicrob. Agents Chemother.* **2005**, *49*, 749–759; c) M. A. Silvers, G. T. Robertson, C. M. Taylor, G. L. Waldrop, *J. Med. Chem.* **2014**, *57*, 8947–8959; d) A. M. Hansen, G. Bonke, C. J. Larsen, N. Yavari, P. E. Nielsen, H. Franzyk, *Bioconjugate Chem.* **2016**, *27*, 863–867; e) S. E. Michalak, S. Nam, D. M. Kwon, D. A. Horne, C. D. A. Vanderwal, *J. Am. Chem. Soc.* **2019**, *141*, 9202–9206.

[5] a) G. Bartoli, M. Bosco, A. Carlone, A. Cavalli, M. Locatelli, A. Mazzanti, P. Ricci, L. Sambri, P. Melchiorre, *Angew. Chem. Int. Ed.* **2006**, *45*, 4966–4970; *Angew. Chem.* **2006**, *118*, 5088–5092; b) C. S. Cucinotta, M. Kosa, P. Melchiorre, A. Cavalli, F. L. Gervasio, *Chem. Eur. J.* **2009**, *15*, 7913–7921.

[6] a) E. Gómez-Torres, D. A. Alonso, E. Gómez-Bengoa, C. Nájera, *Org. Lett.* **2011**, *13*, 6106–6109; b) E. Gómez-Torres, D. A. Alonso, E. Gómez-Bengoa, C. Nájera, *Eur. J. Org. Chem.* **2013**, 1434–1440.

[7] For selected further studies, see: a) Z. Jiang, W. Ye, Y. Yang, C.-H. Tan, *Adv. Synth. Catal.* **2008**, *350*, 2345–2351; b) Y. Qin, G. Yang, L. Yang, J. Li, Y. Cui, *Catal. Lett.* **2011**, *141*, 481–488; c) Y. Qin, W. Zhao, L. Yang, X. Zhang, Y. Cui, *Chirality* **2012**, *24*, 640–645; d) L. Yang, D. Zhou, C. Qu, Y. Cui, *Catal. Lett.* **2012**, *142*, 1405–1410; e) A. Lattanzi, C. De Fusco, A. Russo, A. Poater, L. Cavallo, *Chem. Commun.* **2012**, *48*, 1650–1652; f) W. Zhao, Y. Zhang, C. Qu, L. Zhang, J. Wang, Y. Cui, *Catal. Lett.* **2014**, *144*, 1681–1688; g) H. Zhang, W. Yang, J. Deng, *Polymer* **2015**, *80*, 115–122; h) H. Zhang, Q. Zhang, C. Hong, G. Zou, *Polym. Chem.* **2017**, *8*, 1771–1777; i) V. Kozma, G. Szőllősi, *Mol. Catal.* **2022**, *518*, 112089.

[8] For aryloxide ammonium betaines as enantioselective organocatalysts, see e.g. D. Uraguchi, K. Koshimoto, T. Ooi, *J. Am. Chem. Soc.* **2008**, *130*, 10878–10879.

[9] Selected studies on the general concept of cooperative Lewis acid/Brønsted base catalysis, see e.g.: a) M. Shibasaki, N. Yoshikawa, *Chem. Rev.* **2002**, *102*, 2187–2210; b) H. Sasai, T. Suzuki, S. Arai, T. Arai, M. Shibasaki, *J. Am. Chem. Soc.* **1992**, *114*, 4418–4420; c) H. Sasai, T. Arai, Y. Satow, K. N. Houk, M. Shibasaki, *J. Am. Chem. Soc.* **1995**, *117*, 6194–6198; d) N. Yoshikawa, Y. M. A. Yamada, J. Das, H. Sasai, M. Shibasaki, *J. Am. Chem. Soc.* **1999**, *121*, 4168–4178; e) N. Yamagiwa, H. Qin, S. Matsunaga, M. Shibasaki, *J. Am. Chem. Soc.* **2005**, *127*, 13419–13427; f) Y. S. Kim, S. Matsunaga, J. Das, A. Sekine, T. Ohshima, M. Shibasaki, *J. Am. Chem. Soc.* **2000**, *122*, 6506–6507; g) M. Tokunaga, J. F. Larrow, F. Kakiuchi, E. N. Jacobsen, *Science* **1997**, *277*, 936–938; h) E. F. DiMauro, M. C. Kozlowski, *Org. Lett.* **2001**, *3*, 1641–1644; i) S. Handa, V. Gnanadesikan, S. Matsunaga, M. Shibasaki, *J. Am. Chem. Soc.* **2007**, *129*, 4900–4901.

[10] a) F. Willig, J. Lang, A. C. Hans, M. R. Ringenberg, D. Pfeffer, W. Frey, R. Peters, *J. Am. Chem. Soc.* **2019**, *141*, 12029–12043; b) V. Miskov-Pajic, F. Willig, D. M. Wanner, W. Frey, R. Peters, *Angew. Chem. Int. Ed.* **2020**, *59*, 19873–19877; *Angew. Chem.* **2020**, *132*, 20045–20049.

[11] Recent reviews describing $CH^{\cdot}X$ hydrogen bonds using azolium salts as H-bond donors: a) J. Cai, J. L. Sessler, *Chem. Soc. Rev.* **2014**, *43*, 6198–6213; b) B. Schulze, U. S. Schubert, *Chem. Soc. Rev.* **2014**, *43*, 2522–2571; c) general review on hydrogen bonds: P. M. Pihko, *Hydrogen Bonding in Organic Chemistry*, Wiley-VCH, Weinheim, **2009**.

[12] For the use of azolium salts as enantioselective H-bond donor catalysts, see e.g.: a) K. Ohmatsu, M. Kiyokawa, T. Ooi, *J. Am. Chem. Soc.* **2011**, *133*, 1307–1309; in cooperation with Lewis acids: b) M. Mechler, R. Peters, *Angew. Chem. Int. Ed.* **2015**, *54*, 10303–10307; *Angew. Chem.* **2015**, *127*, 10442–10446; c) J. Schmid, T. Junge, J. Lang, W. Frey, R. Peters, *Angew. Chem. Int. Ed.* **2019**, *58*, 5447–5451; *Angew. Chem.* **2019**, *131*, 5501–5505; d) ref. [10].

[13] For our concept on bifunctional asymmetric Lewis acid/aprotic onium salt catalysis, see e.g.: a) T. Kull, R. Peters, *Angew. Chem. Int. Ed.* **2008**, *47*, 5461–5464; *Angew. Chem.* **2008**, *120*, 5541–5544; b) T. Kull, J. Cabrera, R. Peters,

Chem. Eur. J. **2010**, *16*, 9132–9139; c) P. Meier, F. Broghammer, K. Latendorf, G. Rauhut, R. Peters, *Molecules* **2012**, *17*, 7121–7150; d) F. Broghammer, D. Brodbeck, T. Junge, R. Peters, *Chem. Commun.* **2017**, *53*, 1156–1159; e) D. Brodbeck, F. Broghammer, J. Meisner, J. Klepp, D. Garnier, W. Frey, J. Kästner, R. Peters, *Angew. Chem. Int. Ed.* **2017**, *56*, 4056–4060; *Angew. Chem.* **2017**, *129*, 4115–4119; f) M. Titze, J. Heitkämper, T. Junge, J. Kästner, R. Peters, *Angew. Chem. Int. Ed.* **2021**, *60*, 5544–5553; *Angew. Chem.* **2021**, *133*, 5604–5613; g) J. Heitkämper, J. Herrmann, M. Titze, S. M. Bauch, R. Peters, J. Kästner, *ACS Catal.* **2022**, *12*, 1497–1507.

[14] Deposition Numbers 2191320 (for **S26**), 2191322 (for **C3**), 2191323 (for **3aA**), 2191325 (for **3fA**), 2191326 (for **3gA**), 2191328 (for **3iA**), 2191329 (for **3jA**), 2191332 (for **3nA**), 2191334 (for **3oA**), 2191343 (for **3aC**), 2191344 (for **3aG**), 2191345 (for **5**) und 2191346 (for **10b**) contains the supplementary crystallographic data for this paper. These data are provided free of charge by the joint Cambridge Crystallographic Data Centre and Fachinformationszentrum Karlsruhe Access Structures service.

[15] T. W. Greene, P. G. Wuts, *Protective Groups in Organic Synthesis*, Wiley, New York, **1999**.

[16] a) P. Shah, A. D. Westwell, *J. Enzyme Inhib. Med. Chem.* **2007**, *22*, 527–540; b) J. Wang, M. Sánchez-Roselló, J. L. Aceña, C. del Pozo, A. E. Sorochinsky, S. Fustero, V. A. Soloshonok, H. Liu, *Chem. Rev.* **2014**, *114*, 2432–2506; c) Y. Zhu, J. Han, J. Wang, N. Shibata, M. Sodeoka, V. A. Soloshonok, J. A. S. Coelho, F. D. Toste, *Chem. Rev.* **2018**, *118*, 3887–3964.

[17] a) Z. Jiang, Y. Pan, Y. Zhao, T. Ma, R. Lee, Y. Yang, K.-W. Huang, M. W. Wong, C.-H. Tan, *Angew. Chem. Int. Ed.* **2009**, *48*, 3627–3631; *Angew. Chem.* **2009**, *121*, 3681–3685; b) H. Xue, D. Jiang, H. Jiang, C. W. Kee, H. Hirao, T. Nishimura, M. W. Wong, C.-H. Tan, *J. Org. Chem.* **2015**, *80*, 5745–5752.

[18] Other studies: a) W.-B. Yi, Z. Zhang, X. Huang, A. Tanner, C. Cai, W. Zhang, *RSC Adv.* **2013**, *3*, 18267–18270; b) X. Huang, W.-B. Yi, D. Ahad, W. Zhang, *Tetrahedron Lett.* **2013**, *54*, 6064–6066.

[19] N. Di Iorio, F. Champavert, A. Erice, P. Righi, A. Mazzanti, G. Bencivenni, *Tetrahedron* **2016**, *72*, 5191–5201.

[20] Use of other pronucleophile types: dialdehydes: a) S. Barik, S. Shee, S. Das, R. G. Gonnade, G. Jindal, S. Mukherjee, A. T. Biju, *Angew. Chem. Int. Ed.* **2021**, *60*, 12264–12268; *Angew. Chem.* **2021**, *133*, 12372–12376; b) vinylogous Michael-additions with enones: N. Di Iorio, P. Righi, A. Mazzanti, M. Mancinelli, A. Ciogli, G. Bencivenni, *J. Am. Chem. Soc.* **2014**, *136*, 10250–10253; c) boronic acids: W.-L. Duan, Y. Imazaki, R. Shintani, T. Hayashi, *Tetrahedron* **2007**, *63*, 8529–8536; d) oxindoles: N. Di Iorio, L. Soprani, S. Crotti, E. Marotta, A. Mazzanti, P. Righi, G. Bencivenni, *Synthesis* **2017**, *49*, 1519–1530.

[21] Currently, only a catalytic asymmetric 1,4-addition with oxindoles is known: Y. Zhi, K. Zhao, A. Wang, U. Englert, D. Enders, *Adv. Synth. Catal.* **2017**, *359*, 1867–1871.

[22] a) C. L. Rigby, D. J. Dixon, *Chem. Commun.* **2008**, *32*, 3798–3800; b) S. Tarí, R. Chinchilla, C. Nájera, *Tetrahedron: Asymmetry* **2010**, *21*, 2872–2878; c) S. Tarí, R. Chinchilla, C. Nájera, *Tetrahedron: Asymmetry* **2009**, *20*, 2651–2654.

[23] Alternatively, catalytic asymmetric 1,4-additions to α,β-unsaturated acylphosphonates have been used followed by subsequent alcoholysis of the addition products: H. Jiang, M. W. Paixão, D. Monge, K. A. Jørgensen, *J. Am. Chem. Soc.* **2010**, *132*, 2775–2783.

[24] C. Ding, K. Maruoka, *Synlett* **2009**, 664–666.

[25] a) H. Sasai, T. Arai, M. Shibasaki, *J. Am. Chem. Soc.* **1994**, *116*, 1571–1572; b) H. Sasai, E. Emori, T. Arai, M. Shibasaki, *Tetrahedron Lett.* **1996**, *37*, 5561–5564; c) J. Christoffers, U. Rößler, T. Werner, *Eur. J. Org. Chem.* **2000**, 701–705; d) Y. Hamashima, D. Hotta, M. Sodeoka, *J. Am. Chem. Soc.* **2002**, *124*, 11240–11241; e) T. Ooi, T. Miki, M. Taniguchi, M. Shiraishi, M. Takeuchi, K. Maruoka, *Angew. Chem. Int. Ed.* **2003**, *42*, 3796–3798; *Angew. Chem.* **2003**, *115*, 3926–3928; f) Y. Hamashima, H. Takano, D. Hotta, M. Sodeoka, *Org. Lett.* **2003**, *5*, 3225–3228; g) M. Nakajima, S. Yamamoto, Y. Yamaguchi, S. Nakamura, S. Hashimoto, *Tetrahedron* **2003**, *59*, 7307–7313; h) E. J. Park, M. H. Kim, D. Y. Kim, *J. Org. Chem.* **2004**, *69*, 6897–6899; i) Y. Hamashima, D. Hotta, N. Umebayashi, Y. Tsuchiya, T. Suzuki, M. Sodeoka, *Adv. Synth. Catal.* **2005**, *347*, 1576–1586; j) C. Ogawa, K. Kizu, H. Shimizu, M. Takeuchi, S. Kobayashi, *Chem. Asian J.* **2006**, *1–2*, 121–124; k) J. Comelles, A. Pericas, M. Moreno-Mañas, A. Vallribera, G. Drudis-Solé, A. Lledos, T. Parella, A. Roglans, S. García-Granda, L. Roces-Fernández, *J. Org. Chem.* **2007**, *72*, 2077–2087; l) G. Kumaraswamy, N. Jena, M. N. V. Sastry, M. Padmaja, B. Markondaiah, *Adv. Synth. Catal.* **2005**, *347*, 867–871; m) T. Akiyama, T. Katoh, K. Mori, *Angew. Chem. Int. Ed.* **2009**, *48*, 4226–4228; *Angew. Chem.* **2009**, *121*, 4290–4292; n) C. Xu, L. Zhang, S. Luo, *J. Org. Chem.* **2014**, *79*, 11517–11526.

[26] Selected studies: a) T. Okino, Y. Hoashi, T. Furukawa, X. Xu, Y. Takemoto, *J. Am. Chem. Soc.* **2005**, *127*, 119–125; b) Z. P. Yu, X. H. Liu, L. Zhou, L. L. Lin, X. M. Feng, *Angew. Chem. Int. Ed.* **2009**, *48*, 5195–5198; *Angew. Chem.* **2009**, *121*, 5297–5300; c) M. Furutachi, Z. Chen, S. Matsunaga, M. Shibasaki, *Molecules* **2010**, *15*, 532–544; d) H. Y. Bae, C. E. Song, *ACS Catal.* **2015**, *5*, 3613–3619; e) D. Bécart, V. Diemer, A. Salaün, M. Oiarbide, Y. R. Nelli, B. Kauffmann, L. Fischer, C. Palomo, G. Guichard, *J. Am. Chem. Soc.* **2017**, *139*, 12524–12532; f) J. H. Shim, Y. Hong, J. H. Kim, H. S. Kim, D.-C. Ha, *Catalysts* **2021**, *11*, 1134–1148.

[27] a) J. Burés, *Angew. Chem. Int. Ed.* **2016**, *55*, 2028–2031; *Angew. Chem.* **2016**, *128*, 2068–2071; b) C. D.-T. Nielsen, J. Burés, *Chem. Sci.* **2019**, *10*, 348–353.

[28] T. Satyanarayana, S. Abraham, H. B. Kagan, *Angew. Chem. Int. Ed.* **2009**, *48*, 456–494; *Angew. Chem.* **2009**, *121*, 464–503.

[29] J. Peisach, W. E. Blumberg, *Arch. Biochem. Biophys.* **1974**, *165*, 691–703.

[30] U. Sakaguchi, A. W. Addison, *J. Chem. Soc. Dalton Trans.* **1979**, 600–608.

[31] Z. Damaj, F. Ciscnetti, L. Dupont, E. Henon, C. Policar, E. Guillon, *Dalton Trans.* **2008**, 3235–3245.

[32] P. J. Benites, D. S. Rawat, J. M. Zaleski, *J. Am. Chem. Soc.* **2000**, *122*, 7208–7217.

[33] a) P. Pracht, F. Bohle, S. Grimme, *Phys. Chem. Chem. Phys.* **2020**, *22*, 7169–7192; b) S. Grimme, *J. Chem. Theory Comput.* **2019**, *15*, 2847–2862; c) J. Kästner, J. M. Carr, T. W. Keal, W. Thiel, A. Wander, P. Sherwood, *J. Phys. Chem. A* **2009**, *113*, 11856–11865; d) P. Sherwood, A. H. de Vires, M. F. Guest, G. Schreckenbach, C. R. A. Catlow, S. A. French, A. A. Sokol, S. T. Bromley, W. Thiel, A. J. Turner, S. Billeter, F. Terstegen, S. Thiel, J. Kendrick, S. C. Rogers, J. Casci, M. Watson, F. King, E. Karlsen, M. Sjøvoll, A. Fahmi, A. Schäfer, C. Lennartz, *J. Mol. Struct.* **2003**, *632*, 1–28; e) S. Metz, J. Kästner, A. A. Sokol, T. W. Keal, P. Sherwood, *Wiley Interdiscip. Rev. Comput. Mol. Sci.* **2014**, *4*, 101–110; f) C. Bannwarth, S. Ehlert, S. Grimme, *J. Chem. Theory Comput.* **2019**, *15*, 1652–1671; g) TURBOMOLE V7 2015, a development of the University of Karlsruhe and Forschungszentrum Karlsruhe GmbH, 1989–2007, TURBOMOLE GmbH, since 2007; can be found under http://www.turbomole.com; h) S. Grimme, J. G. Brandenburg, C. Bannwarth, A. Hansen, *J. Chem. Phys.* **2015**, *143*, 054107–054117; i) S. Grimme, J. Antony, S. Ehrlich, H. Krieg, *J. Chem. Phys.*

2010, *132*, 154104–154117; j) S. Grimme, S. Ehrlich, L. Goerigk, *J. Comput. Chem.* **2011**, *32*, 1456–1465; k) A. D. Becke, *Phys. Rev. A* **1988**, *38*, 3098–3100; l) C. Lee, W. Yang, R. G. Parr, *Phys. Rev. B* **1988**, *37*, 785–789; m) A. D. Becke, *J. Chem. Phys.* **1993**, *98*, 5648–5652; n) F. Weigend, R. Ahlrichs, *Phys. Chem. Chem. Phys.* **2005**, *7*, 3297–3305; o) F. Weigend, *Phys. Chem. Chem. Phys.* **2006**, *8*, 1057–1065; p) A. Klamt, G. Schüürmann, *J. Chem. Soc. Perkin Trans. 2* **1993**, 799–805.

[34] A. Bondi, *J. Phys. Chem.* **1964**, *68*, 441–451.

[35] D. A. Evans, M. C. Kozlowski, J. A. Murry, C. S. Burgey, K. R. Campos, B. T. Connell, R. J. Staples, *J. Am. Chem. Soc.* **1999**, *121*, 669–685.

Manuscript received: November 28, 2022
Accepted manuscript online: January 18, 2023
Version of record online: February 14, 2023